The de Haas–van Alphen effect and the Fermi surface in $CePt_3Si$ and $LaPt_3Si$

2004 J. Phys.: Condens. Matter 16 L287

(http://iopscience.iop.org/0953-8984/16/23/L02)

INSTITUTE OF PHYSICS PUBLISHING JOURNAL OF PHYSICS: CONDENSED MATTER

J. Phys.: Condens. Matter **16** (2004) L287–L296 PII: S0953-8984(04)77706-1

LETTER TO THE EDITOR

The de Haas–van Alphen effect and the Fermi surface in $CePt_3Si$ and $LaPt_3Si$

Shin Hashimoto[1], Takashi Yasuda[1], Tetsuo Kubo[1], Hiroaki Shishido[1], Taiki Ueda[1], Rikio Settai[1,4], Tatsuma D Matsuda[2], Yoshinori Haga[2], Hisatomo Harima[3] and Yoshichika Ōnuki[1,2]

[1] Graduate School of Science, Osaka University, Toyonaka, Osaka 560-0043, Japan
[2] Advanced Science Research Center, Japan Atomic Energy Research Institute, Tokai, Ibaraki 319-1195, Japan
[3] The Institute of Scientific and Industrial Research, Osaka University, Ibaraki, Osaka 567-0047, Japan

E-mail: settai@phys.sci.osaka-u.ac.jp

Received 14 March 2004
Published 28 May 2004
Online at stacks.iop.org/JPhysCM/16/L287
DOI: 10.1088/0953-8984/16/23/L02

Abstract

We have carried out a de Hass–van Alphen (dHvA) experiment for the recently discovered $CePt_3Si$, which is the first heavy fermion superconductor without inversion symmetry in the tetragonal crystal structure, together with a dHvA experiment for a non-4f reference compound $LaPt_3Si$. As for $LaPt_3Si$, several dHvA branches were observed. Among them, the two main dHvA branches with the dHvA frequency (the cyclotron effective mass) of 1.10×10^8 Oe ($1.4\ m_0$) and 8.41×10^7 Oe ($1.5\ m_0$) were found to be well explained from the FLAPW energy band calculations, corresponding to bands 64- and 63-multiply-connected hole Fermi surfaces, respectively. On the other hand, the dHvA frequencies of 10^7 Oe in $CePt_3Si$ are small in magnitude, although the corresponding cyclotron masses of 10–20 m_0 are extremely large.

The recently discovered superconductor $CePt_3Si$ is unique, possessing a few characteristics [1]. Superconductivity is realized in the long-range antiferromagnetic ordering. The Néel temperature is 2.2 K, while the superconducting transition temperature is 0.75 K. Both transitions were observed clearly in the specific heat measurement. The electronic specific heat coefficient γ is large, 300–400 mJ K^{-2} mol^{-1}. In the previous cerium-based heavy fermion superconductors including a prototype superconductor $CeCu_2Si_2$ and a quasi-two dimensional superconductor $CeCoIn_5$ with a large γ value of 1000 mJ K^{-2} mol^{-1}, superconductivity occurs in the non-magnetic or antiferromagnetically spin-fluctuating state [2–4]. Another example is $CeIn_3$ under pressure [4–6]. At ambient pressure, the Néel temperature in $CeIn_3$ is $T_N = 10$ K

[4] Author to whom any correspondence should be addressed.

and the ordered moment is 0.5 μ_B/Ce. With increasing pressure P, T_N decreases smoothly as a function of pressure and becomes zero around a critical pressure $P_c \simeq 2.7$ GPa where superconductivity sets in below 0.2 K.

We note here that superconductivity in the uranium compounds is very different from that in the cerium compounds. In the uranium-based heavy fermion superconductors such as UPd_2Al_3, it is clear that the 5f-electrons are itinerant and also contribute to the magnetic moment at the uranium site [7, 8]. This dual nature of the f electrons is not realized in the cerium compounds. Namely, the antiferromagnetic state is due to the localized-4f electron and the conduction electrons are mainly due to the non-4f valence electrons.

These phenomena result from the competition between the Ruderman–Kittel–Kasuya–Yosida (RKKY) interaction and the Kondo effect [9]. The RKKY interaction enhances the long-range magnetic order, where the f electron with the magnetic moment is treated as the localized electron and the indirect f–f interaction is mediated by the spin polarization of the conduction electrons. On the other hand, the Kondo effect quenches the magnetic moment of the localized f electron by the spin polarization of the conduction electrons, producing the singlet state with the binding energy $k_B T_K$, where T_K is called the Kondo temperature, which leads to the heavy fermion state with an extremely large effective mass at lower temperatures than T_K.

The existence of inversion symmetry in the crystal structure is believed to be a favourable factor for superconductivity. The absence of superconductivity in, for example, the ferromagnet MnSi has been tentatively attributed to a lack of inversion symmetry in its crystal structure [10]. $CePt_3Si$ is the first heavy fermion superconductor lacking a centre of symmetry [1]. The crystal structure of $CePt_3Si$ is tetragonal, space group $P4mm$ (No. 99) with $a = 4.072$ Å and $c = 5.442$ Å.

The present purpose is to present the electronic states of $CePt_3Si$ and also of the non-4f reference compound $LaPt_3Si$. We have carried out a de Haas–van Alphen (dHvA) experiment of $CePt_3Si$ and $LaPt_3Si$. The experimental results are compared to the results of FLAPW energy band calculations.

Single crystals of $CePt_3Si$ and $LaPt_3Si$ were obtained by the Bridgeman method and/or mineralization. Polycrystals were first made by arc-melting under argon gas atmosphere using 99.95%-pure Ce, 99.99% (4N)-La, 4N-Pt and 5N-Si. The polycrystals were sealed in a molybdenum crucible, which was heated up to 1450 °C and cooled down to room temperature.

The residual resistivity ρ_0 and the residual resistivity ratio RRR ($=\rho_{RT}/\rho_0$) for the current along [001] were $\rho_0 = 0.9$ $\mu\Omega$ cm and RRR $= 106$ in $CePt_3Si$ and $\rho_0 = 0.4$ $\mu\Omega$ cm and RRR $= 74$ in $LaPt_3Si$, indicating high-quality single crystal samples. These values are compared to $\rho_0 = 5$ $\mu\Omega$ cm and RRR $= 18$ in the polycrystal sample in [1]. We note that $LaPt_3Si$ also becomes superconductive below 0.7 K.

For these samples, we carried out the dHvA experiment by the usual field-modulation method at low temperatures down to 30 mK and at high magnetic fields up to 170 kOe. Figure 1(a) shows the typical dHvA oscillation and its fast Fourier transform (FFT) spectrum for the field along the [001] direction in $LaPt_3Si$. Several dHvA branches named α, β, ... are observed.

The detected dHvA signal V_{osc} can be simply written as follows [11]:

$$V_{osc} = A \sin\left(\frac{2\pi F}{H} + \phi\right), \tag{1}$$

$$A \propto J_2(x) T H^{-1/2} \left|\frac{\partial^2 S}{\partial k_H^2}\right|^{-1/2} \frac{\exp(-\alpha m_c^* \frac{T_D}{H})}{\sinh(\alpha m_c^* \frac{T}{H})}, \tag{2}$$

$$\alpha = \frac{2\pi^2 c k_B}{e\hbar}, \tag{3}$$

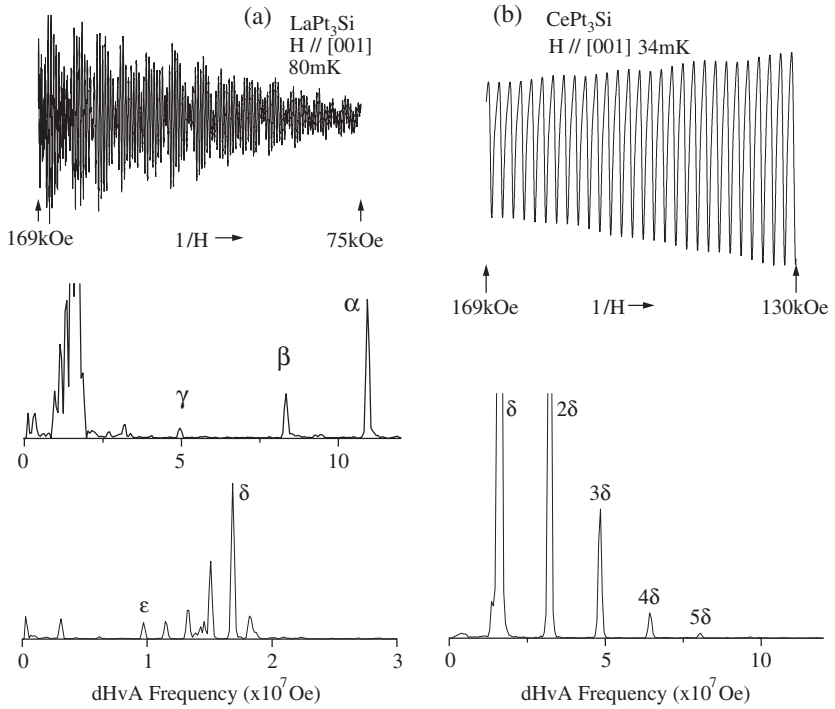

Figure 1. (a) Typical dHvA oscillation and its FFT spectrum for $H \parallel [001]$ (c-axis) in (a) $LaPt_3Si$ and (b) $CePt_3Si$.

where the dHvA frequency F ($=c\hbar S_F/2\pi e$) is proportional to the extremal (maximum or minimum) cross-sectional area of the Fermi surface S_F. The amplitude A is related to the Bessel function $J_2(x)$ ($x = 2\pi Fh/H^2$), the modulation field h, the temperature T, the magnetic field H, the cyclotron effective mass m_c^*, the Dingle temperature T_D ($=\hbar\tau^{-1}/2\pi k_B$), which is inversely proportional to the scattering lifetime τ, and the curvature factor of the Fermi surface $\left|\partial^2 S/\partial k_H^2\right|^{-1/2}$.

We determined the cyclotron mass m_c^* from the temperature dependence of the dHvA amplitude A and also the Dingle temperature T_D or the scattering lifetime τ from the field dependence of the dHvA amplitude. These values are shown in table 1. The mean free path ℓ in table 1 was estimated from the following simple relations: $S_F = \pi k_F^2$, $\hbar k_F = m_c^* v_F$ and $\ell = v_F\tau$, where the wavenumber k_F is half of the caliper dimension of the circular cross-sectional area S_F and v_F is the Fermi velocity. For example, the cyclotron mass and mean free path in branch α are 1.4 m_0 and 2400 Å, respectively, indicating a high-quality sample.

On the other hand, the detected dHvA branches possess small dHvA frequencies in $CePt_3Si$. One dHvA branch is mainly observed for $H \parallel [001]$, as shown in figure 1(b), and the others are harmonics. The dHvA frequency is 1.60×10^7 Oe. The corresponding cyclotron mass is 2.8 m_0. For $H \parallel [100]$, three dHvA branches are observed, as shown in figure 2(c). The corresponding cyclotron masses are extremely large, 11–23 m_0, because the dHvA frequencies of 10^7 Oe are small in magnitude, as summarized in table 2.

The dHvA experiments were performed for all the field directions for $LaPt_3Si$ and $CePt_3Si$. Figure 2(a) shows the angular dependence of the dHvA frequency in $LaPt_3Si$. The main dHvA branches named α and β, together with branch γ, are observed in a narrow angle region centred at the [001] direction. The corresponding dHvA frequencies are 1.10×10^8, 8.41×10^7 and

Table 1. dHvA frequency F, the cyclotron mass m_c^*, the Dingle temperature T_D and the mean free path ℓ in $LaPt_3Si$.

Branch	F (10^7 Oe)	m_c^* (m_0)	T_D (K)	ℓ (Å)
		$H \parallel [001]$		
α	11.0	1.4	2.5	2400
β	8.41	1.5		
γ	4.91	2.4		
	1.81			
δ	1.68	1.2	2.5	1000
	1.51	1.1		
	1.33	1.1		
	1.15	1.0		
ε	0.97	1.0		
	0.31	0.96		
		$H \parallel [100]$		
	9.18	2.5		
	2.84	2.0		
	2.75	0.76		
ζ	2.38	0.44	3.6	2400
	2.02	0.78		
	1.70	0.77		
	1.63	1.2		
η	1.10	0.84		
	1.05	0.77		
	0.61	1.3		
		$H \parallel [110]$		
	8.38	2.9		
	7.94	1.8		
	7.73	2.3		
	7.42	1.7		
	6.91	1.7	2.1	1800
	1.88	1.4	1.2	1200
	0.74			
	0.31	1.3	1.0	1000

Table 2. dHvA frequency F, the cyclotron mass m_c^*, the Dingle temperature T_D and the mean free path ℓ in $CePt_3Si$.

Branch	F (10^7 Oe)	m_c^* (m_0)	T_D (K)	ℓ (Å)
		$H \parallel [001]$		
δ	1.60	2.8	0.43	2600
	1.37			
		$H \parallel [100]$		
	1.83	11	0.11	2700
	1.64	14	0.20	1200
	1.49	23	0.11	1200

4.91×10^7 Oe, respectively. A dHvA branch with 9.18×10^7 Oe is also observed around [100]. The dHvA frequencies in the other branches are small, and are observed around the principal

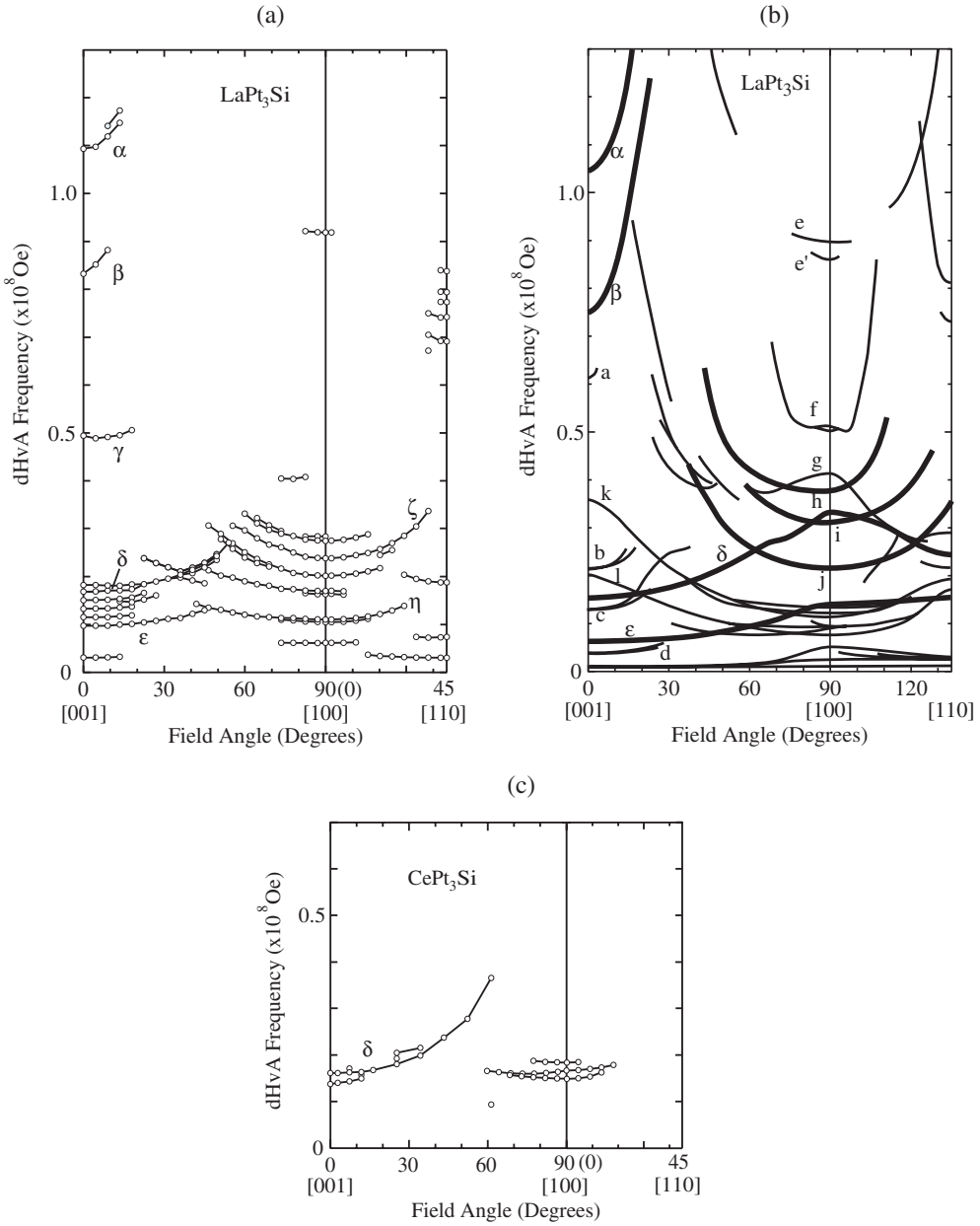

Figure 2. Angular dependence of (a) the dHvA frequency in $LaPt_3Si$, (b) the theoretical dHvA frequency in $LaPt_3Si$, and (c) the dHvA frequency in $CePt_3Si$.

field directions. These results indicate that the main Fermi surfaces are the multiply-connected Fermi surfaces. Figure 2(b) shows the corresponding angular dependence of the theoretical dHvA frequency in $LaPt_3Si$, which will be described later. We also show in figure 2(c) the angular dependence of the dHvA frequency in $CePt_3Si$. The detected dHvA branches are small in number, as mentioned above.

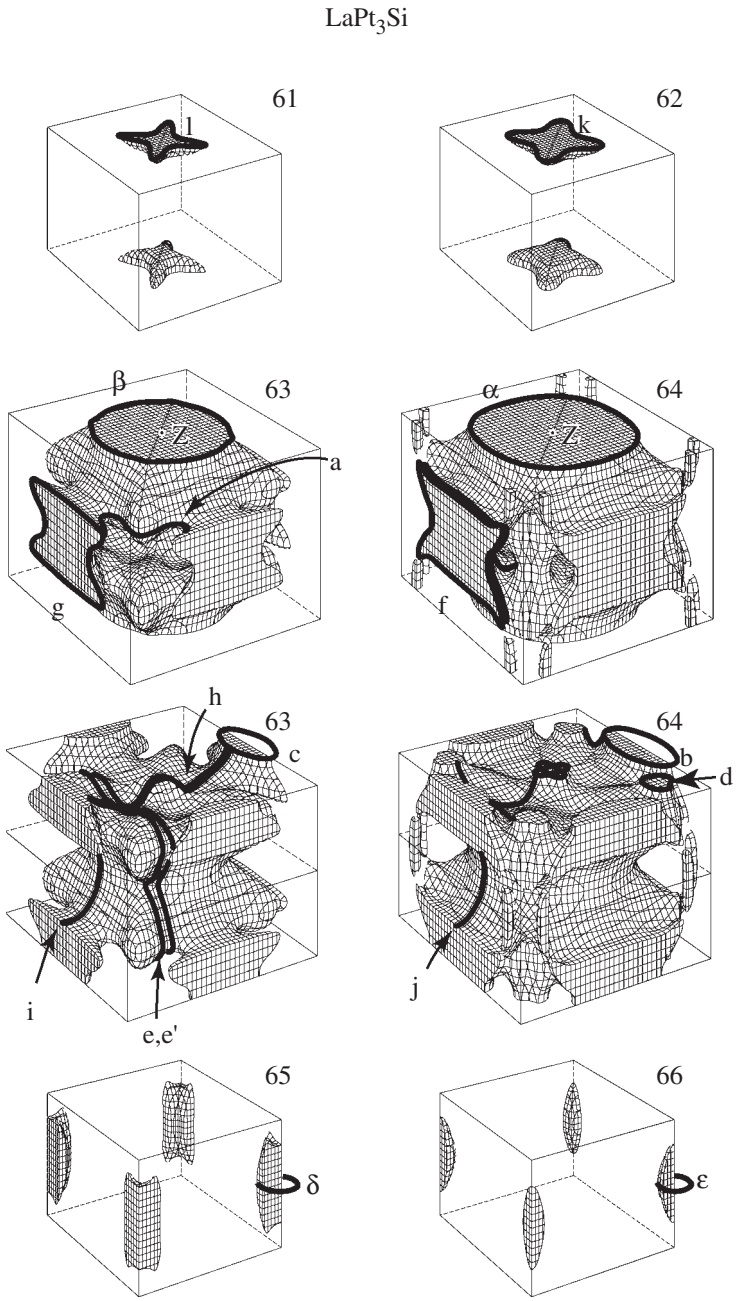

Figure 3. Bands 61–64 hole Fermi surfaces and bands 65 and 66 electron Fermi surfaces in $LaPt_3$ Si. The Fermi surfaces in the third line are centred at the Z point, compared to the Γ-centred Fermi surfaces in the second line.

For $LaPt_3Si$ and $CePt_3Si$, the band structure calculations were carried out using a full potential LAPW method. The calculations were performed by using the local density approximation (LDA) for the exchange correlation potential within the formula proposed by Gunnarsson and Lundqvist [12]. Here, we used the program codes TSPACE [13] and

KANSAI-03. The scalar relativistic effects were taken into account for all electrons, and the spin–orbit interactions were included self-consistently for all valence electrons as in a second variational procedure.

The lattice constants used for the calculations are $a = 4.072$ Å and $c = 5.442$ Å [1]. Muffin-tin (MT) radii are set as $0.4020a$ for La/Ce, $0.2716a$ for Pt and $0.2500a$ for Si. Core electrons (Xe-core minus $5s^2 5p^6$ for La/Ce, Xe-core minus $5p^6$ for Pt, Ne-core for Si) are calculated inside the MT spheres in each self-consistent step. The $5s^2$ electrons on La/Ce and $5p^6$ electrons on Pt are calculated as valence electrons by using the second energy window.

The LAPW basis functions are truncated at $|\boldsymbol{k} + \boldsymbol{G}_i| \leqslant 4.46 \times 2\pi/\boldsymbol{a}$, corresponding to 503 LAPW functions at the Γ point. The sampling points are uniformly distributed in the irreducible 1/8th of the Brillouin zone (IBZ), 315 $\boldsymbol{k}$-points (divided by 16, 16, 12) both for the potential convergence and for the final band structure. The density of states at the Fermi level is calculated as 7.66 mJ K^{-2} mol^{-1} for $LaPt_3Si$ and 11.30 mJ K^{-2} mol^{-1} for $CePt_3Si$. The value of 7.66 mJ K^{-2} mol^{-1} in $LaPt_3Si$ is close to the experimental value of 9 mJ K^{-2} mol^{-1} [1].

Figures 3 and 2(b) show the Fermi surface and the corresponding theoretical angular dependence of the dHvA frequency in $LaPt_3Si$, respectively. Based on these results, the main detected dHvA branches are as follows.

(1) Branch α ($F = 1.10 \times 10^8$ Oe and $m_c^* = 1.4\ m_0$) corresponds to an orbit α with a theoretical dHvA frequency $F = 1.05 \times 10^8$ Oe and a band mass $m_b = 0.91\ m_0$ in the band 64-hole Fermi surface, as shown in figure 3 and table 3.
(2) Branch β ($F = 8.41 \times 10^7$ Oe and $m_c^* = 1.5\ m_0$) corresponds to an orbit β with $F = 7.50 \times 10^7$ Oe and $m_b = 0.98\ m_0$ in the band 63-hole Fermi surface.
(3) Branch δ ($F = 1.68 \times 10^7$ Oe and $m_c^* = 1.2\ m_0$) corresponds to an orbit δ with $F = 1.54 \times 10^7$ Oe and $m_b = 0.72\ m_0$ in the band 65-electron Fermi surface, although it is not observed in the whole angle region. This is mainly due to a curvature factor problem of the Fermi surface.
(4) Branch ε ($F = 9.7 \times 10^6$ Oe and $m_c^* = 1.0\ m_0$) corresponds to an orbit ε with $F = 6.3 \times 10^6$ Oe and $m_b = 0.51\ m_0$ in the band 66-electron Fermi surface, although it is also not observed in the whole angle region, similarly to branch δ.
(5) Several dHvA branches are observed around [001]. Three orbits named h, i, j, shown by thick solid lines in figure 2(b), are theoretically detectable because of a small curvature $\left|\partial^2 S/\partial k_{H^2}\right|$ of these orbits in the bands 63- and 64-Fermi surfaces. We cannot, however, identify the observed branches with the theoretical orbits.

From these results, the detected main dHvA branches in $LaPt_3Si$ are well explained by the results of the present FLAPW band calculations.

Unlike in $LaPt_3Si$, the detected dHvA branches in $CePt_3Si$ are small in number. We will discuss the origin of the dHvA branches in $CePt_3Si$ on the basis of a 4f-localized band model, namely the Fermi surface of a non-4f reference compound $LaPt_3Si$, because it orders antiferromagnetically. From the recent neutron scattering experiment [14], it was clarified that the magnetic moments of the 4f electrons at the cerium sites orient ferromagnetically in the (001) plane and are stacked antiferromagnetically along the [001] direction, indicating an antiferromagnetic propagation vector $q = (0\,0\,1/2)$. The magnetic moment is, however, small: 0.2 μ_B/Ce. Moreover, the CEF excitations were clearly observed at 1 and 24 meV, indicating three doublet 4f-levels.

The dHvA branch with 1.60×10^7 Oe for $H \parallel [001]$ in $CePt_3Si$ might correspond to the branch δ with 1.68×10^7 Oe in $LaPt_3Si$ from the magnitude and angular dependence of the dHvA frequency. The three dHvA branches for $H \parallel [100]$ in $CePt_3Si$ are not identified because the dHvA branches for $H \parallel [100]$ in $LaPt_3Si$ are also not clear in origin.

Table 3. Theoretical dHvA frequency F and the band mass m_b in $LaPt_3Si$.

		[001]			[100]			[110]	
		F (10^7 Oe)	m_b (m_0)		F (10^7 Oe)	m_b (m_0)		F (10^7 Oe)	m_b (m_0)
Band 61 (hole)	l	2.01	0.91		0.94	0.59		1.71	0.79
					0.76	0.55			
Band 62 (hole)	k	3.60	0.73		1.35	0.55		1.93	0.78
					1.15	0.55			
Band 63 (hole)				e	8.99	1.51			
				e'	1.15	0.55			
								8.15	1.74
	β	7.50	0.98						
	a	6.12	4.40						
				g	4.14	1.59			
				h	3.78	1.13			
				h	3.76	1.15			
				i	3.11	0.45			
								2.17	0.98
	c	1.29	0.79						
					0.92	0.72			
Band 64	α	10.5	0.91						
								7.30	1.33
				f	5.11	2.55			
				f	5.02	3.06			
					3.09	1.19			
					3.06	1.69			
				j	2.15	0.36	j	3.55	0.75
	b	2.15	1.33						
					1.22	0.46			
								0.95	0.60
					0.81	1.11			
		0.40	0.78						
	d	0.37	0.67						
Band 65 (electron)	δ	1.54	0.72		3.32	2.17		2.89	1.71
								2.44	1.09
Band 66 (electron)	ε	0.63	0.51		1.40	0.72		1.53	0.81

The main Fermi surfaces in $CePt_3Si$ were thus not determined experimentally. The reason is as follows. From the neutron scattering experiment mentioned above, the antiferromagnetic Brillouin zone in $CePt_3Si$ becomes half of the Brillouin zone in $LaPt_3Si$ along the [001] direction. The branches α and β might be not affected by this flat Brillouin zone, although these branches are not observed experimentally. The cyclotron masses in both branches are expected to become extremely large in $CePt_3Si$, because the γ value is 300–400 mJ K^{-2} mol^{-1} in $CePt_3Si$ and 9 mJ K^{-2} mol^{-1} in $LaPt_3Si$ [1]. The cyclotron mass in $CePt_3Si$ is therefore estimated as 45–60 m_0 in branch α and 50–65 m_0 in branch β for $H \parallel [001]$, because the corresponding cyclotron mass in $LaPt_3Si$ is 1.4 and 1.5 m_0, respectively. Moreover, the steep curvature of the Fermi surface for both branches might also become a strong reduction factor of the dHvA amplitude. These are the main reasons why the main dHvA branches α and β are not observed in $CePt_3Si$.

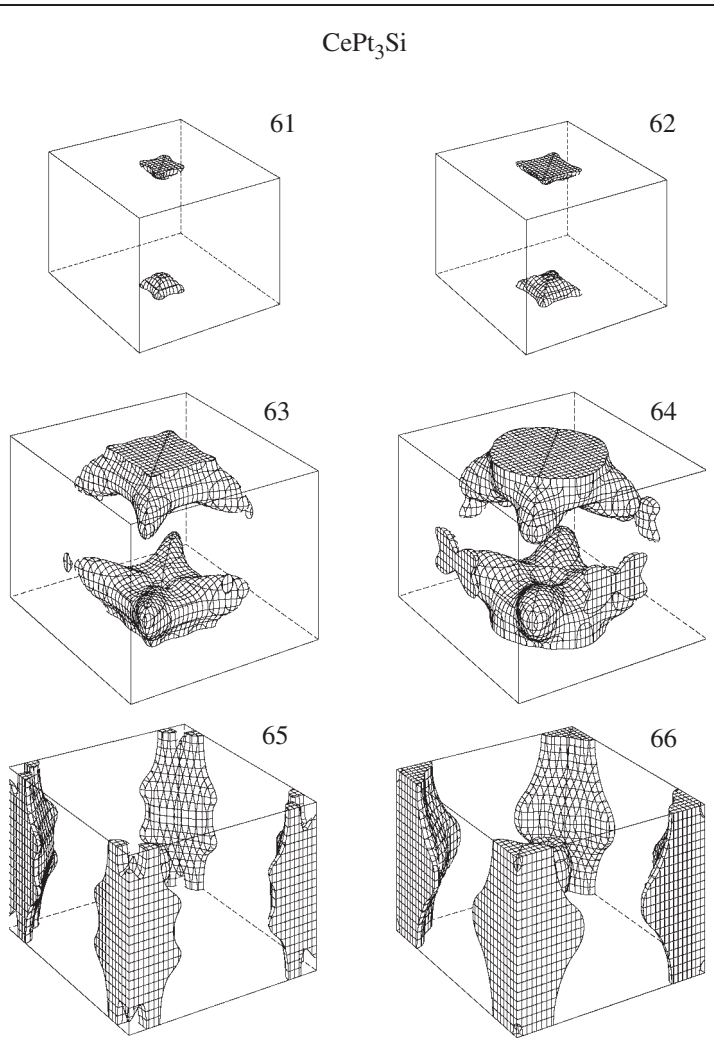

Figure 4. Bands 61–64 hole Fermi surfaces, and bands 65 and 66 electron Fermi surfaces in the 4f-itinerant band calculations for $CePt_3Si$.

The detected cyclotron mass of the three dHvA branches for $H \parallel [100]$ in $CePt_3Si$ is extremely large, 11–23 m_0, because the corresponding dHvA frequency is small: (1.5–1.8) $\times$ 10^7 Oe. Here the cyclotron mass with the similar dHvA frequency in $LaPt_3Si$ is less than 1 m_0. It is strange that the cyclotron mass of branch δ for $H \parallel [001]$ in $CePt_3Si$ is not large, 2.8 m_0, which is compared to 1.2 m_0 for the corresponding branch δ in $LaPt_3Si$. This means that the mass renormalization is most likely anisotropic, depending on the Fermi surface, and branch δ due to a small band 65-Fermi surface does not obey the mass renormalization condition.

Here we present in figure 4 the theoretical Fermi surface under the assumption that the 4f electron is itinerant and $CePt_3Si$ is in the paramagnetic state. In this case, $CePt_3Si$ becomes a compensated metal with equal volumes of electron and hole Fermi surfaces. A main orbit in the band 64-hole Fermi surface possesses a small curvature, most likely detectable in the dHvA experiment. Moreover, several orbits in the corrugated cylindrical Fermi surfaces in bands 65 and 66 electron Fermi surfaces might also be observed experimentally. We cannot,

however, apply this Fermi surface model to the present dHvA result of $CePt_3Si$ because it orders antiferromagnetically.

We will summarize the dHvA experiment of $CePt_3Si$ and $LaPt_3Si$. The two main dHvA branches named α and β in $LaPt_3Si$, which are observed around [001], are well explained by the results of FLAPW energy band calculations. The corresponding theoretical Fermi surface are multiply-connected, indicating a three-dimensional electronic state. The topology of the Fermi surface in $CePt_3Si$ is most likely similar to that of $LaPt_3Si$, because the 4f electron is localized from the results of neutron scattering experiment. In fact, one small Fermi surface in $CePt_3Si$ is similar to that in $LaPt_3Si$. The two main Fermi surfaces named α and β in $LaPt_3Si$ are, however, not observed in $CePt_3Si$, which is most likely due to an extremely large cyclotron mass of about 50 m_0 and a steep curvature of the Fermi surfaces.

The present work was financially supported by Grant-in-Aid for Creative Scientific Research(15GS0123) and for Scientific Research of Priority Area from the Ministry of Education, Culture, Sports, Science and Technology.

References

[1] Bauer E, Hilscher G, Michor H, Paul Ch, Scheidt E W, Gribanov A, Seropegin Yu, Noël H, Sigrist M and Rogl P 2004 *Phys. Rev. Lett.* **92** 027003
[2] Steglich F, Aarts J, Bredl C D, Lieke W, Meschede D, Franz W and Schäfer H 1979 *Phys. Rev. Lett.* **43** 1892
[3] Petrovic C, Pagliuso P G, Hundley M F, Movshovich R, Sarrao J L, Thompson J D, Fisk Z and Monthoux P 2001 *J. Phys.: Condens. Matter* **13** L337
[4] Kitaoka Y, Kawasaki Y, Mito T, Kawasaki S, Zheng G-q, Ishida K, Aoki D, Haga Y, Settai R, Ōnuki Y, Geibel C and Steglich F 2002 *J. Phys. Chem. Solids* **63** 1141
[5] Mathur N D, Grosche F M, Julian S R, Walker I R, Freye D M, Haselwimmer R K W and Lonzarich G G 1998 *Nature* **394** 39
[6] Knebel G, Braithwaite D, Canfield P C, Lapertot G and Flouquet J 2002 *Phys. Rev.* B **65** 024425
[7] Inada Y, Yamagami H, Haga Y, Sakurai K, Tokiwa Y, Honma T, Yamamoto E, Ōnuki Y and Yanagisawa T 1999 *J. Phys. Soc. Japan* **68** 3643
[8] Sato N K, Aso N, Miyake K, Shiina R, Thalmeier P, Varelogiannis G, Geibel C, Steglich F, Fulde P and Komatsubara T 2001 *Nature* **410** 340
[9] Doniach S 1977 *Valence Instabilities and Related Narrow Band Phenomena* ed R D Parks (New York: Plenum) p 169
[10] Pfleiderer C, McMullan G J, Julian S R and Lonzarich G G 1997 *Phys. Rev.* B **55** 8330
[11] Ōnuki Y and Hasegawa A 1995 *Handbook on the Physics and Chemistry of Rare Earth* vol 20, ed K A Gschneidner Jr and L Eyring (Amsterdam: Elsevier Science) p 1
[12] Gunnarsson O and Lundqvist B I 1976 *Phys. Rev.* B **13** 4274
[13] Yanase A 1995 *Fortran Program for Space Group* 1st edn (Tokyo: Shokabo) (in Japanese)
[14] Metoki N, Kaneko K, Matsuda T D, Galatanu A, Takeuchi T, Hashimoto S, Ueda T, Settai R and Ōnuki Y 2004 *J. Phys.: Condens. Matter* **16** L207